Annular Bilayer Magnetoelectric Composites: Theoretical Analysis

Mingsen Guo and Shuxiang Dong

***Abstract*—The laminated bilayer magnetoelectric (ME) composites consist of magnetostrictive and piezoelectric layers are known to have giant ME coefficient due to the high coupling efficiency in bending mode. In our previous report, the bar-shaped bilayer composite has been investigated by using a magnetoelectric-coupling equivalent circuit. Here, we propose an annular bilayer ME composite, which consists of magnetostrictive and piezoelectric rings. This composite has a much lower resonance frequency of bending mode compared with its radial mode. In addition, the annular bilayer ME composite is expected to respond to vortex magnetic field as well as unidirectional magnetic field. In this paper, we investigate the annular bilayer ME composite by using impedance-matrix method and predict the ME coefficients as a function of geometric parameters of the composites.**

I. Introduction

Interest in the magnetoelectric (ME) effect can be dated back to the 1950s [1]. However, during the past decade, multiferroic ME materials have attracted renewed interest for both their fundamental physical properties and potential applications as memories, sensors, transducers, and so on [2]–[4]. Multiferroic materials are classified as either single-phase or multiphase multiferroics. However, because spin and/or charge ordering temperatures remain far below room temperature, and only in response to high applied magnetic or electric fields, single-phase multiferroic compounds [5] remain more a scientific curiosity than viable engineering materials.

In comparison to single-phase multiferroics, the multiphase composites, generally consisting of a ferromagnetic phase and a ferroelectric phase, are able to demonstrate considerably stronger ME couplings at room temperature and therefore have begun to receive intense interest [6]–[12]. The ME effect in ME composite is known as a product tensor property [4], which results from the cross interaction between different orderings of the 2 phases in the composite. Neither the piezoelectric nor the magnetic phase has the ME effect, but composites composed of these 2 phases have remarkable ME effect. Thus, the ME effect is a result of the product of the magnetostrictive effect (magnetic/mechanical effect) in the magnetic phase and the piezoelectric effect (mechanical/electrical effect) in the piezoelectric one. Due to a strong elastic coupling between magnetostrictive and piezoelectric layers, laminated composites (constructed by bonding the 2 layers together) have been experimentally found to exhibit a giant ME coefficient of > 1 V/cm Oe [9], [10], [13]. ME composites can be used as transducers for energy conversion between magnetic field energy and electric field energy; and therefore, they have potential applications as highly sensitive magnetic sensors [14], [15], magnetic field energy and mechanical energy-harvesting devices [16], voltage transformers [17], current-voltage converters or gyrators [18], and microwave devices [19], [20].

It is known that the frequency affects significantly the ME coupling in the laminated composites. When the laminated composite operates in the resonance mode, its ME effect could be enhanced greatly, generally yielding an ME voltage output of nearly 2 orders of magnitude over that of the nonresonant ME laminates [21]. To date, many experiments and calculations have been performed to optimize the resonant ME output for the laminates. Very promising results have been obtained in resonance modes including the longitudinal mode and radial mode. However, a problem that caused attention is that the operating frequencies are generally high, which could bring significant eddy current loss for the magnetostrictive phase, especially for the large magnetostrictive rare earth alloys such as Terfenol-D, resulting in an inefficient ME energy conversion. Accordingly, a magnetostrictive/piezoelectric laminated bilayer composite with a bar shape that operates in bending-resonance mode was proposed and has been further studied by many researchers due to its simple structure and low-resonance-frequency characteristics [22]–[27]. Here, we propose an annular bilayer ME composite, which consists of a magnetostrictive ring and a piezoelectric ring. This composite has a much lower resonance frequency of bending mode compared with its radial mode. In addition, similar to a symmetrical ring-type ME lamination (magnetostrictive/piezoelectric/magnetostrictive) proposed by Dong *et al.* [15], [28], the annular bilayer ME composite is also expected to respond to a vortex magnetic field as well as a unidirectional magnetic field. In this paper, we will further develop the 1-D theory from our previous work [27] into 2-D theory and investigate the ME property of the annular bilayer ME composite.

II. Theoretical Analysis

The analysis for laminated magnetostrictive/piezoelectric annular bilayer composites should take into account

Manuscript received September 14, 2009; accepted October 19, 2009. This work was supported by the National Basic Research Program of China (973 Program, Grant No. 2009CB623303) and China Postdoctoral Science Foundation (Grant No. 20090450218).

The authors are with the Department of Advanced Materials & Nanotechnology, College of Engineering, Peking University, Beijing, China (e-mail: sdongpku@gmail.com).

Digital Object Identifier 10.1109/TUFFC.2010.1428

0885–3010/$25.00 © 2010 IEEE

Authorized licensed use limited to: Peking University. Downloaded on February 24,2010 at 22:07:09 EST from IEEE Xplore. Restrictions apply.

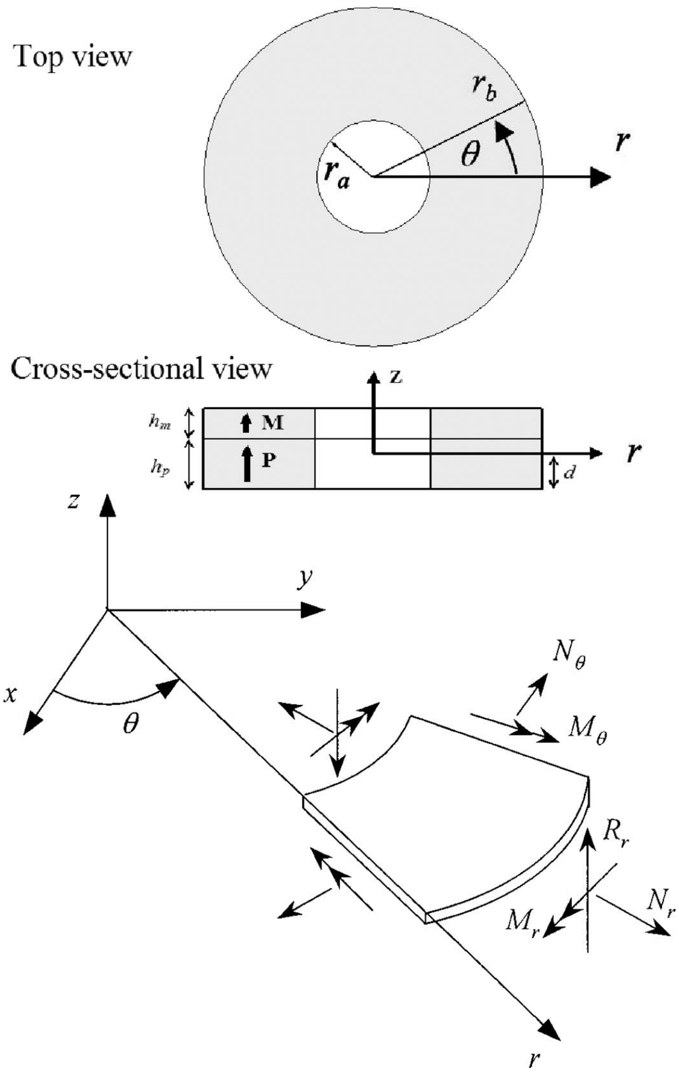

Fig. 1. Schematic diagram of the annular bilayer magnetoelectric composite and stress analysis in the differential element.

both the extensional and flexural deformations. By ignoring the coupling between extensional and flexural motions, the differential equations for the extensional and flexural vibration can be derived, respectively, [29], [30]. In [30], by using impedance and admittance matrices, Ha and Kim presented a theoretical model for the analysis of an asymmetrical piezoelectric annular bimorph in dynamic harmonic motion. Here, we modify this model for analyzing the ME response of a laminated magnetostrictive/piezoelectric annular bilayer composite.

A. Working Modes

We consider a laminated annular bilayer ME composite that consists of magnetostrictive and piezoelectric phases as shown in Fig. 1. The piezoelectric layer has electrodes on the top and bottom main surfaces, and it is polarized along the thickness direction (z axis direction). A dc-biasing magnetic field H and a small-magnitude ac magnetic field δH are applied along the thickness direction. The application of ac magnetic field δH induces forced oscillation of the composite via magnetostrictive effect and generates a voltage in the piezoelectric layer through the piezoelectric effect. Because of the nonlinear property of magnetostrictive materials, an appropriate biasing magnetic H is applied to maximize the ME effect. Due to the asymmetrical characteristic of the bilayer composite, nonuniformly distributed (along thickness direction) stress causes extensional deformation as well as flexural deformation. The extensional deformation dominates in radial vibration resonance mode, whereas the flexural deformation dominates in bending vibration resonance mode.

B. Constitutive Equations

The ME effect in laminated composites is a product property. Two sets of linear constitutive equations (for small signal excitation) are required to describe the ME product property. For the bilayer modeling, 2 important assumptions were made: 1) the interface between layers is continuous, and they do not slip with respect to one another; and 2) the thickness is small compared with the lateral dimension.

When frequency is far below the first resonance frequency of thickness extensional vibration mode, the stress T_{zz} are small compared with T_{rr} and $T_{\theta\theta}$. ($T_{zz} = 0$). The piezomagnetic constitutive equations for the magnetostrictive phase are

$$S_{rrm} = s_{11m}^{H} T_{rrm} + s_{12m}^{H} T_{\theta\theta m} + d_{31m} H_0 \tag{1a}$$

$$S_{\theta\theta m} = s_{12m}^{H} T_{rrm} + s_{11m}^{H} T_{\theta\theta m} + d_{31m} H_0 \tag{1b}$$

where H_0 is the external magnetic field strength; T_{rrm}, $T_{\theta\theta m}$, S_{rrm}, and $S_{\theta\theta m}$ are the radial and circumferential normal stresses and strains in magnetostrictive layer; the subscript m means magnetostrictive phase; s_{11m}^{H}, s_{12m}^{H}, and d_{31m} are the elastic compliance at constant magnetic field and the transverse piezomagnetic constant, respectively.

The piezoelectric constitutive equations are

$$S_{rrp} = s_{11p}^{D} T_{rrp} + s_{12p}^{D} T_{\theta\theta p} + g_{31p} D_z \tag{2a}$$

$$S_{\theta\theta p} = s_{12p}^{D} T_{rrp} + s_{11p}^{D} T_{\theta\theta p} + g_{31p} D_z \tag{2b}$$

$$E_z = -g_{31p}(T_{rrp} + T_{\theta\theta p}) + \beta_{33}^{T} D_z \tag{2c}$$

where D_z and E_z are the electric displacement and electric field; T_{rrp}, $T_{\theta\theta p}$, S_{rrp}, and $S_{\theta\theta p}$ are the radial and circumferential normal stresses and strains in piezoelectric layer; the subscript p means piezoelectric phase; s_{11p}^{D}, s_{12p}^{D}, g_{31p}, and β_{33}^{T} are the elastic compliance at constant electric displacement, the transverse piezoelectric constant, and the dielectric stiffness at constant stress, respectively.

C. Equation of Motion, General Solution, and Boundary Condition

Under the assumption of axial symmetry, all the mechanical and electromagnetic components are independent

Authorized licensed use limited to: Peking University. Downloaded on February 24,2010 at 22:07:09 EST from IEEE Xplore. Restrictions apply.

of θ. Based on the Kirchhoff assumption and the axial symmetric condition, the displacements are supposed to be [30]

$$u_r(r,z) = u_R(r) - z\frac{\partial u_z}{\partial r}, \quad u_\theta(r,z) = 0, \quad u_z(r,z) = w(r); \tag{3}$$

u_R is the radial extensional displacement, i.e., the radial displacement u_R at the neutral plane ($z = 0$) that will be determined later; w is the deflection displacement along z axis. In [31], Yang pointed out that the neutral axis cannot be used as a reference axis in the modeling of asymmetrically laminated beams or plates with elastic and piezoelectric layers. The location of the neutral axis is load dependant, and it consists of points that do not fall in a straight line in the reference state. Here, no external force load is applied, and the magnetically induced displacement is small, so the concept of neutral plane is acceptable. The strain-displacement relationship can then be expressed as

$$S_{rr} = \frac{\partial u_r}{\partial r} = \frac{\partial u_R}{\partial r} - z\frac{\partial^2 w}{\partial r^2}, \quad S_{\theta\theta} = \frac{u_r}{r} = \frac{u_R}{r} - z\frac{1}{r}\frac{\partial w}{\partial r}. \tag{4}$$

It is known that every point on the electrode of piezoelectric layer has an equal voltage. Integrating electric field E_z over the thickness of the piezoelectric layer, the coupling voltage on the 2 electrode surfaces of the piezoelectric ring can be determined as

$$V = \int_{\text{piezo}} E_z \mathrm{d}z. \tag{5}$$

So, we obtain the electric displacement as a function of voltage and displacement

$$D_z = \frac{V}{\bar{\beta}_{33} h_p} - \gamma_{pN}\left(\frac{\partial u_R}{\partial r} + \frac{u_R}{r}\right) - \gamma_{pM}\left(\frac{\partial^2 w}{\partial r^2} + \frac{1}{r}\frac{\partial w}{\partial r}\right), \tag{6}$$

where

$$\gamma_{pN} = -\frac{g_{31p}}{\bar{\beta}_{33} s^D_{11p}(1-\sigma_p)}, \quad \sigma_p = -s^D_{12p}/s^D_{11p},$$
$$\bar{\beta}_{33} = \beta^T_{33}\left(1 + \frac{2g^2_{31p}}{\beta^T_{33} s^D_{11p}(1-\sigma_p)}\right), \tag{7}$$

$$\gamma_{pM} = -\gamma_{pN}\left(\frac{h_p}{2} - d\right); \tag{8}$$

d is the distance between the neutral plane and the outer surface of piezoelectric layer.

Using (6), performing the integration yields the expression for the electric charge of piezoelectric layer (per unit angle):

$$Q = \int_{r_a}^{r_b} D_z r \mathrm{d}r = C_0 V - \gamma_{pN} u_R\Big|_{r=r_a}^{r=r_b} - \gamma_{pM} r\frac{\partial w}{\partial r}\Big|_{r=r_a}^{r=r_b}, \tag{9}$$

where $C_0 = (r_b^2 - r_a^2)/2\bar{\beta}_{33} h_p$ is the static capacitance of the piezoelectric layer (per unit angle).

The decoupled equations of extensional and bending motions of the annular bilayer ME composite have the form (see Appendix A for details)

$$\frac{\partial^2 u_R}{\partial r^2} + \frac{1}{r}\frac{\partial u_R}{\partial r} - \frac{u_R}{r^2} + \lambda_N^2 u_R = 0, \tag{10a}$$

$$\left(\frac{\partial^2}{\partial r^2} + \frac{1}{r}\frac{\partial}{\partial r}\right)^2 w - \lambda_M^4 w = 0. \tag{10b}$$

The general solutions to (10) are

$$u_R(r) = \Phi_N^T A_N, \tag{11a}$$

$$w(r) = \Phi_M^T A_M, \tag{11b}$$

where

$$\Phi_N = (J_1(\lambda_N r) \quad Y_1(\lambda_N r))^T, \tag{12a}$$

$$\Phi_M = (J_0(\lambda_M r) \quad Y_0(\lambda_M r) \quad I_0(\lambda_M r) \quad K_0(\lambda_M r))^T. \tag{12b}$$

The coefficient vectors A_N, A_M are to be determined using the boundary conditions.

The forces and moments at the boundary are

$$F_N = B_N^F A_N + C_N^H H_0 + C_N^V V, \tag{13a}$$

$$F_M = B_M^F A_M + C_M^H H_0 + C_M^V V. \tag{13b}$$

The displacements at the boundary are

$$u_N = B_N^u A_N, \tag{14a}$$

$$u_M = B_M^u A_M. \tag{14b}$$

D. Impedance Matrix and ME Coefficient

For the derivation of impedance matrix, velocity vectors U_N and U_M and electric current I are used instead of the displacement vectors u_N and u_M and the charge Q, respectively. Because we are considering all the physical quantities in the harmonic response, the following relations are used:

$$U_N = i\omega u_N, \quad U_M = i\omega u_M, \tag{15a}$$

$$I = i\omega Q, \tag{15b}$$

where the electric current I is the current per unit angle flows through the piezoelectric layer. Eliminating the coef-

Authorized licensed use limited to: Peking University. Downloaded on February 24,2010 at 22:07:09 EST from IEEE Xplore. Restrictions apply.

$$\begin{pmatrix} F_N \\ F_M \\ V \end{pmatrix} = \begin{bmatrix} Z_N + C_N^V Z_C (C_N^V)^T & C_N^V Z_C (C_M^V)^T & C_N^V Z_C \\ & Z_M + C_M^V Z_C (C_M^V)^T & C_M^V Z_C \\ \text{sym.} & & Z_C \end{bmatrix} \begin{pmatrix} U_N \\ U_M \\ I \end{pmatrix} + H_0 \begin{pmatrix} C_N^H \\ C_M^H \\ 0 \end{pmatrix} \quad (18)$$

TABLE I. Material Parameters of Terfenol-D and PZT Ceramics.

	Density (kg/m^3)	Elastic constants ($\times$ 10^{-12} m^2/N)		Piezoelectric/magnetic constants	Dielectric constant
		s_{11}^D	s_{12}^D		$\varepsilon_{33}^T/\varepsilon_0$
PZT (Pz26)[1]	7700	11.6	−5.74	g_{31} −0.0109 Vm/N	1330
		s_{11}^H	s_{12}^H		
Terfenol-D[2]	9230	125	−37.5	d_{31} 5.8 × 10^{-9} Wb/N	

[1]Cited from *Ferroperm Piezoceramics* [33].
[2]Cited from [28].

ficient vectors A_N and A_M from (13) and (14), then using (A40) and (15), we obtain

$$\begin{pmatrix} F_N \\ F_M \\ -I \end{pmatrix} = \begin{bmatrix} Z_N & & C_N^V \\ & Z_M & C_M^V \\ \text{sym.} & & -Z_C^{-1} \end{bmatrix} \begin{pmatrix} U_N \\ U_M \\ V \end{pmatrix} + H_0 \begin{pmatrix} C_N^H \\ C_M^H \\ 0 \end{pmatrix}, \quad (16)$$

where

$$Z_N = \frac{1}{i\omega} B_N^F (B_N^u)^{-1}, \quad (17a)$$

$$Z_M = \frac{1}{i\omega} B_M^F (B_M^u)^{-1}, \quad (17b)$$

$$Z_C = \frac{1}{i\omega C_0}. \quad (17c)$$

The exchange of the current for the voltage in (16) easily yields the impedance matrix in (18), see above. The exchange of force vectors for velocity vectors in (18) yields the admittance matrix:

$$\begin{pmatrix} U_N \\ U_M \\ I \end{pmatrix} = \begin{bmatrix} Y_N & & -Y_N C_N^V \\ & Y_M & -Y_M C_M^V \\ \text{sym.} & & Y_E \end{bmatrix} \begin{pmatrix} F_N - H_0 C_N^H \\ F_M - H_0 C_M^H \\ V \end{pmatrix}, \quad (19)$$

which enables us to calculate the mechanical and electrical responses of the composite due to harmonic excitation by either forces at boundary or magnetic (electric) field. The electrical admittance matrices in (19) are defined as

$$Y_N = (Z_N)^{-1}, \quad (20a)$$

$$Y_M = (Z_M)^{-1}, \quad (20b)$$

$$Y_E = (C_N^V)^T Y_N C_N^V + (C_M^V)^T Y_M C_M^V + i\omega C_0. \quad (20c)$$

In case of no external loads ($F_N = 0$, $F_M = 0$, $H_0 = 0$), Y_E represents the admittance of electrical port. The poles and zeros of Y_E give the characteristic equations that yield the resonance frequency ω_r and the antiresonance frequency ω_a.

The ME voltage response of the annular bilayer ME composite can be derived from (19) using different boundary conditions (free-free, clamped-free, free-clamped, each at the inner and outer radii). Here, for simplicity, we only consider the free-free boundary condition ($F_N = 0$, $F_M = 0$). Under open-circuit condition, electric current I from the piezoelectric layer is 0. Using (19), we get the following relationship:

$$V = -H_0 \frac{(C_N^V)^T Y_N C_N^H + (C_M^V)^T Y_M C_M^H}{i\omega C_0 + (C_N^V)^T Y_N C_N^V + (C_M^V)^T Y_M C_M^V}. \quad (21)$$

The ME voltage coefficient is defined as

$$\alpha_{\mathrm{ME}} = \left| \frac{dV}{dH_0} \right|. \quad (22)$$

III. Results and Discussion

We consider an annular ME composite made of Terfenol-D/PZT bilayer. The properties of the magnetostrictive and piezoelectric materials are listed in Table I. The inner radius (r_a) is 2.5 mm, and the outer radius (r_b) is 10 mm. The thicknesses of the Terfenol-D and PZT are both 0.5 mm. Using (20c), the first bending vibration resonance frequency of 6.8 kHz and the first radial extensional vibration resonance frequency of 64.3 kHz are obtained for free-free boundary condition. To check the results, simple structural modal analysis based on 3-D finite element method is performed. Fig. 2 shows the mode shapes of the first bending vibration resonance mode and the first radial mode at 6559 Hz and 63678 Hz, respectively. (In the simulation, a partial annular model with 30° is created.) Comparison between the analytical and FEM results shows good agreement. Because the extensional

Authorized licensed use limited to: Peking University. Downloaded on February 24,2010 at 22:07:09 EST from IEEE Xplore. Restrictions apply.

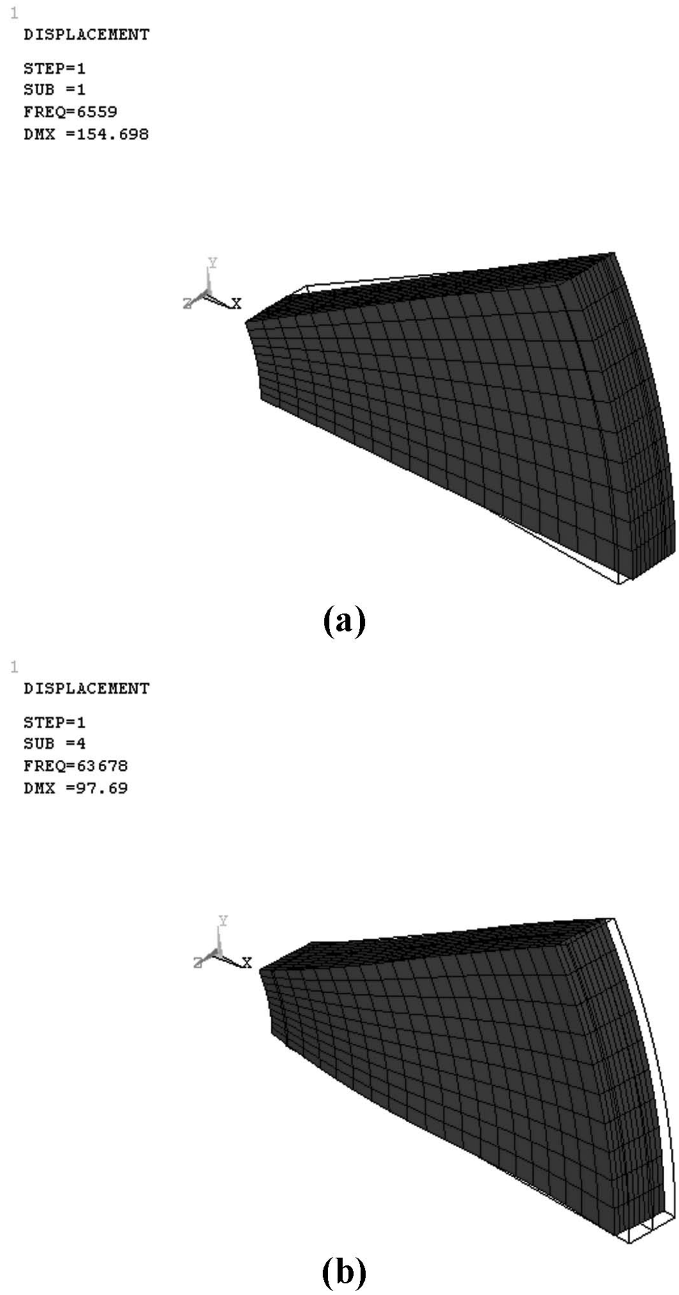

Fig. 2. Structural modal analysis results of (a) the first bending vibration mode and (b) the first radial extensional vibration mode of the Terfenol-D/PZT annular bilayer composite in free boundary condition.

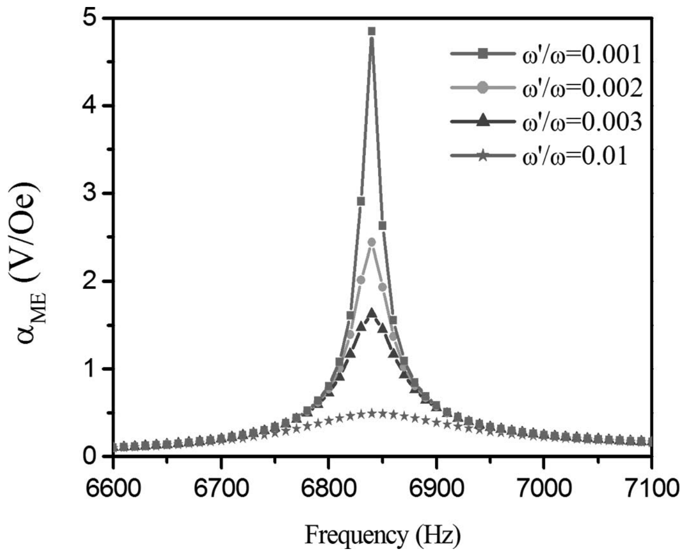

Fig. 3. Magnetoelectric voltage coefficient-frequency relationship of the Terfenol-D/PZT bilayer composite near the resonance frequency of the first bending mode.

and bending motions cannot be completely decoupled (as discussed in Appendix A), discrepancy between the analytical solution and FEM numerical simulation exists.

Fig. 3 shows the calculated ME coefficients in neighborhood of the first bending-resonance frequency. Resonance losses should be taken into account by a complex frequency $\omega - i\omega'$. This figure shows that the ME coefficient at resonance is strongly related to loss [21]. A value of $\omega'/\omega = 0.003$ is used to predict ME voltage, and good agreements between calculation and experimental data are obtained ($\alpha_{\mathrm{Resonance}}/\alpha_{\mathrm{Low\text{-}frequency}} \approx 50$) [23]. As we can see from Fig. 3, the ME coefficient (with $\omega'/\omega = 0.003$) is expected to be 1.63 V/Oe (32.6 V/cm Oe). The calculated results are in the same order with experimental data [23].

In the annular bilayer ME composite, the thickness ratio $n = h_m/(h_m + h_p)$ should be taken into account for the design of the device. We calculated the ME coefficients at resonance frequency with various thickness ratios. In calculation, the value of ω'/ω is set to 0.003. The results are shown in Fig. 4. From Fig. 4 we can see some features: 1) If the magnetostrictive plate thickness is reduced to zero, i.e., $n \to 0$, the ME coefficient is zero. This means there is no bending or stretching. 2) The α_{ME}^{V} of the bending mode is maximum at $n \approx 0.8$. It is noted that the optimum thickness ratio n for maximum resonance ME voltage coefficient will change when using different material elastic compliances. It is noted that the thickness ratio dependence of the ME coefficient in the annular bilayer composite is similar to the case of the bar-shaped bilayer composite [27].

Fig. 5 shows the ME coefficients at low frequency (1 Hz) of the annular (circular) bilayer ME composites with different sizes. In calculation, the total thickness of the bilayer composite is fixed to 1 mm ($h_m + h_p = 1$ mm). From Fig. 5, we can see that the ratio of radius (r_a/r_b) has no effect on the low-frequency ME response. The thickness ratio dependence of the low-frequency ME coefficient is similar to that in a bar-shaped bilayer composite [27]. Results of ME voltage coefficient, α_{ME} vs. n reveal double maximums due to fact that the strain induced consists of 2 components: radial extensional and flexural. Because the mean flexural strain in piezoelectric layer is of opposite sign relative to radial extensional strain, the 2 types of strains combine to produce suppression of ME voltage coefficient at $n \approx 0.7$ and double maximums in the $\alpha_{\mathrm{ME}} - n$ curve. Fig. 5 also shows the thickness ratio n dependence of low-frequency ME field coefficient (dE/dH). The ME field coefficient increases monotonically from zero for $n = 0$ to a finite value (~11 V/cm Oe) for $n = 1$.

Authorized licensed use limited to: Peking University. Downloaded on February 24,2010 at 22:07:09 EST from IEEE Xplore. Restrictions apply.

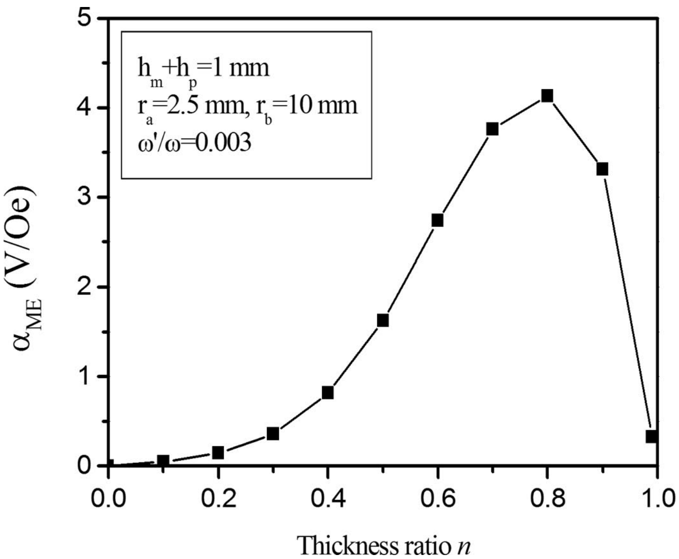

Fig. 4. Calculated thickness ratio, $n = h_m/(h_m + h_p)$, dependence of resonance magnetoelectric coefficients of Terfenol-D/PZT bilayer composite in the first bending mode. The total thickness $(h_m + h_p)$ is 1 mm, and ω'/ω is fixed to 0.003.

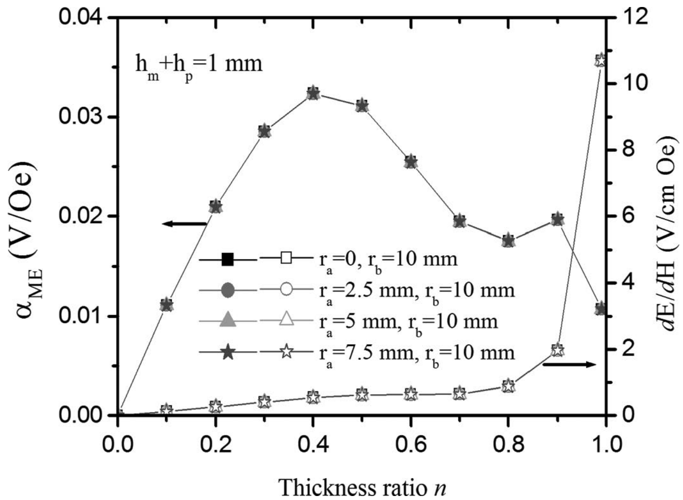

Fig. 5. Calculated thickness ratio n dependence of low-frequency (quasi-static) magnetoelectric coefficients of Terfenol-D/PZT bilayer composite with various inner radius. The total thickness of bilayer is 1 mm.

It is known that for a magnetic material in an external magnetic field, effect of demagnetization will take place [32]. None of the above discussion takes this effect into consideration. In an external magnetic field, a magnetic material affects the distribution of magnetic flux in its interior and near outer space. The magnetic flux density B_z in the magnetic phase is

$$B_z = \mu_{33} H_z = \mu_{33}(H_0 - H_z{}'), \tag{23}$$

where $H_z{}'$ is the value of demagnetization field $\vec{H}'(x, y, z)$ in z direction, μ_{33} is the magnetic permeability. If we simply ignore the distribution of demagnetization field, we have

$$\frac{B_z}{\mu_0 H_0} = \frac{1}{N_d}, \tag{24}$$

where N_d is the demagnetizing factor. The value of N_d depends mainly on the aspect ratio of the magnetic material. The magnetically induced strain $d_{31m}H_0$ in (1) should be replaced by

$$d_{\mathrm{eff}} H_0 = d_{31m} H_z = g_{31m} B_z = \frac{\mu_0 d_{31m}}{\mu_{33}^T N_d} H_0, \tag{25}$$

where d_{eff} is effective piezomagnetic constant, and $g_{31m} = d_{31m}/\mu_{33}^T$. For rings with $h_m \ll r_b - r_a$, B_z inside the magnetic material is nearly the same as that in the free space ($B_z = \mu_0 H_0$, $N_d = 1$). So the effective piezomagnetic constant d_{eff} equals $d_{31m}\mu_0/\mu_{33}^T$.

We note that the annular bilayer ME composite is expected to respond to vortex magnetic field as well as unidirectional magnetic field. In [15] and [28], a symmetrical ring-type ME laminated composite of 2 magnetostrictive layers and 1 piezoelectric layer was presented for the measurement of alternating current (ac) vortex magnetic field at frequencies between sub-hertz and kilohertz. For the circumferentially magnetized and circumferentially polarized (C-C) ME mode, an equivalent circuit has been developed for analysis of ME response. The asymmetrical bilayer ME composite has a simpler structure compared with the symmetrical composite. However, theoretical analysis is more complicated for the asymmetrical bilayer ME composite in vortex magnetic field, and it is yet to be explored.

We need to indicate that the impedance-matrix approach may be also useful for modeling the ME behavior of low-dimensional thin-film ME composite, because their working modes are quite similar. But in thin-film ME composite, the thicknesses of electrodes are comparable to that of magnetostrictive and piezoelectric layers, so the effect of electrode thickness cannot be ignored. The present model should be modified to be applicable for thin-film multilayer composite if electrode thickness cannot be ignored.

IV. Conclusion

In summary, we propose an annular bilayer ME composite that consists of magnetostrictive and piezoelectric rings. This composite has a much lower resonance frequency of bending mode compared with its radial mode and has a potential application as ac current sensors and magnetic sensors. To analyze properties of the annular bilayer composite, we develop an impedance-matrix method, which is useful for predicting the ME coefficients of the composite. The calculated resonance frequencies are compared with results of FEM analysis, and good agreement is achieved. The enhancement of ME voltage coefficient in neighborhood of the first bending-resonance frequency is

Authorized licensed use limited to: Peking University. Downloaded on February 24,2010 at 22:07:09 EST from IEEE Xplore. Restrictions apply.

illustrated. The dependences of resonance-enhanced ME coefficient and low-frequency (quasistatic) ME coefficient on geometric factors (ratio of inner radius to outer radius and ratio of layer thickness) are also calculated and discussed.

Appendix A

Equation of Motion, General Solution, and Boundary Condition

The analysis of annular bilayer ME composite is performed using a similar method as described in [30]. By using impedance and admittance matrices, Ha and Kim presented a theoretical model for the analysis of an asymmetrical piezoelectric annular bimorph in dynamic harmonic motion. The conjugate parameters of the admittance and impedance matrices were derived using the variation principle. Both the extensional and flexural motions were considered in deriving the motional equations and boundary conditions. Here, we present the modified results for ME analysis. For detailed derivation procedure, please read [30].

The extensional force N, flexural moment M, and shear force R_r as shown in Fig. 1 are given by

$$N_r = \int T_{rr} \mathrm{d}z, \quad N_\theta = \int T_{\theta\theta} \mathrm{d}z, \tag{A1}$$

$$M_r = -\int T_{rr} z \mathrm{d}z, \quad M_\theta = -\int T_{\theta\theta} z \mathrm{d}z. \tag{A2}$$

$$rR_r = -\frac{\partial (rM_r)}{\partial r} + M_\theta. \tag{A3}$$

Inserting (1), (2), (4), and (6) into (A1) and (A2) yields the following expressions for the extensional forces and the flexural moments:

$$\begin{pmatrix} N_r \\ N_\theta \\ M_r \\ M_\theta \end{pmatrix} = \begin{bmatrix} A_{11} & A_{12} & B_{11} & B_{12} \\ A_{21} & A_{22} & B_{21} & B_{22} \\ B_{11} & B_{12} & D_{11} & D_{12} \\ B_{21} & B_{22} & D_{21} & D_{22} \end{bmatrix} \begin{pmatrix} \dfrac{\partial u_R}{\partial r} \\ \dfrac{u_R}{r} \\ \dfrac{\partial^2 w}{\partial r^2} \\ \dfrac{1}{r}\dfrac{\partial w}{\partial r} \end{pmatrix} + \begin{pmatrix} N_r^* \\ N_\theta^* \\ M_r^* \\ M_\theta^* \end{pmatrix}, \tag{A4}$$

where the equivalent extensional forces N_r^*, N_θ^* and the equivalent flexural moments M_r^*, M_θ^* that result from the magnetic and electric fields are

$$N_r^* = N_\theta^* = \gamma_{pN} V + \gamma_{mN} H_0, \tag{A5}$$

$$M_r^* = M_\theta^* = \gamma_{pM} V + \gamma_{mM} H_0, \tag{A6}$$

where

$$\gamma_{mN} = -\frac{d_{31m}}{s_{11m}^H (1-\sigma_m)} h_m, \quad \sigma_m = -\frac{s_{12m}^H}{s_{11m}^H}, \tag{A7}$$

$$\gamma_{mM} = -\gamma_{mN}\left(\frac{h_m}{2} + h_p - d\right). \tag{A8}$$

The stiffness matrices A_{ij}, B_{ij}, and D_{ij} in (A4) are defined as

$$A_{11} = A_{22} = h_p\left(\bar{c}_{11p} - \frac{g_{31p}^2}{\bar{\beta}_{33}\left(s_{11p}^D(1-\sigma_p)\right)^2}\right) + h_m \bar{c}_{11m}, \tag{A9}$$

$$A_{12} = A_{21} = h_p\left(\sigma_p \bar{c}_{11p} - \frac{g_{31p}^2}{\bar{\beta}_{33}\left(s_{11p}^D(1-\sigma_p)\right)^2}\right) + \sigma_m h_m \bar{c}_{11m}, \tag{A10}$$

$$B_{11} = B_{22} = -h_p\left(\frac{h_p}{2} - d\right)\left(\bar{c}_{11p} - \frac{g_{31p}^2}{\bar{\beta}_{33}\left(s_{11p}^D(1-\sigma_p)\right)^2}\right) - h_m\left(\frac{h_m}{2} + h_p - d\right)\bar{c}_{11m}, \tag{A11}$$

$$B_{12} = B_{21} = -h_p\left(\frac{h_p}{2} - d\right)\left(\sigma_p \bar{c}_{11p} - \frac{g_{31p}^2}{\bar{\beta}_{33}\left(s_{11p}^D(1-\sigma_p)\right)^2}\right) - \sigma_m h_m\left(\frac{h_m}{2} + h_p - d\right)\bar{c}_{11m}, \tag{A12}$$

$$D_{11} = D_{22} = \Omega_1 + \Omega_2 + \Omega_3, \tag{A13}$$

$$D_{12} = D_{21} = \Omega_1 \sigma_p + \Omega_2 + \Omega_3 \sigma_m, \tag{A14}$$

where

$$\Omega_1 = \bar{c}_{11p}\left[\frac{h_p^3}{12} + h_p\left(\frac{h_p}{2} - d\right)^2\right], \quad \bar{c}_{11p} = 1/[s_{11p}^D(1-\sigma_p^2)], \tag{A15}$$

$$\Omega_2 = -\frac{g_{31p}^2}{\bar{\beta}_{33}\left[s_{11p}^D(1-\sigma_p)\right]^2} h_p\left(\frac{h_p}{2} - d\right)^2, \tag{A16}$$

$$\Omega_3 = \bar{c}_{11m}\left[\frac{h_m^3}{12} + h_m\left(\frac{h_m}{2} + h_p - d\right)^2\right], \quad \bar{c}_{11m} = \frac{1}{s_{11m}^H(1-\sigma_m^2)}. \tag{A17}$$

The differential equations of the extensional and flexural motions can be decoupled by eliminating the matrix B_{ij} [30]. The distance between the neutral plane and the outer surface of piezoelectric layer, d is determined so that $B_{11}(= B_{22})$ vanish

$$d = \frac{h_p}{2} + \frac{\bar{c}_{11m} h_m (h_m + h_p)}{2(c'_p h_p + \bar{c}_{11m} h_m)}, \tag{A18}$$

where

Authorized licensed use limited to: Peking University. Downloaded on February 24,2010 at 22:07:09 EST from IEEE Xplore. Restrictions apply.

$$B_N^F = A_{11}\begin{bmatrix} -\lambda_N r_a J_N^{0a} + J_N^{1a} - \alpha J_N^{1a} & -\lambda_N r_a Y_N^{0a} + Y_N^{1a} - \alpha Y_N^{1a} \\ \lambda_N r_b J_N^{0b} - J_N^{1b} + \alpha J_N^{1b} & \lambda_N r_b Y_N^{0b} - Y_N^{1b} + \alpha Y_N^{1b} \end{bmatrix}, \tag{A30}$$

$$B_M^F = D_{11}\lambda_M^2 \begin{pmatrix} r_a J_M^{0a} - \beta J_M^{1a} & r_a Y_M^{0a} - \beta Y_M^{1a} & -r_a I_M^{0a} + \beta I_M^{1a} & -r_a K_M^{0a} - \beta K_M^{1a} \\ \lambda_M r_a J_M^{1a} & \lambda_M r_a Y_M^{1a} & \lambda_M r_a I_M^{1a} & -\lambda_M r_a K_M^{1a} \\ -r_b J_M^{0b} + \beta J_M^{1b} & -r_b Y_M^{0b} + \beta Y_M^{1b} & r_b I_M^{0b} - \beta I_M^{1b} & r_b K_M^{0b} + \beta K_M^{1b} \\ -\lambda_M r_b J_M^{1b} & -\lambda_M r_b Y_M^{1b} & -\lambda_M r_b I_M^{1b} & \lambda_M r_b K_M^{1b} \end{pmatrix}, \tag{A31}$$

$$c'_p = \bar{c}_{11p} - \frac{g_{31p}^2}{\bar{\beta}_{33}\left[s_{11p}^D(1-\sigma_p)\right]^2}.$$

If the Poisson's ratios of all the layers are the same, B_{12} is close to zero and the distance d is uniquely determined. However, in other cases, B_{12} is ignored, and the decoupling is performed approximately.

The decoupled equations of extensional and bending motions of the annular bilayer ME composite have the form

$$\frac{\partial^2 u_R}{\partial r^2} + \frac{1}{r}\frac{\partial u_R}{\partial r} - \frac{u_R}{r^2} + \lambda_N^2 u_R = 0, \tag{A19}$$

$$\left(\frac{\partial^2}{\partial r^2} + \frac{1}{r}\frac{\partial}{\partial r}\right)^2 w - \lambda_M^4 w = 0, \tag{A20}$$

where the parameters λ_N and λ_M are functions of the angular frequency ω, each defined as

$$\lambda_N = \left(\frac{\rho_p h_p + \rho_m h_m}{A_{11}}\right)^{1/2}\omega, \qquad \lambda_M = \left(\frac{\rho_p h_p + \rho_m h_m}{D_{11}}\right)^{1/4}\omega^{1/2}; \tag{A21}$$

ρ_m and ρ_p are the density of magnetostrictive and piezoelectric phase, respectively.

The general solution of (A19) and (A20) can be written as

$$u_R(r) = \Phi_N^T A_N, \tag{A22}$$

$$w(r) = \Phi_M^T A_M, \tag{A23}$$

where

$$\Phi_N = \left(J_1(\lambda_N r) \quad Y_1(\lambda_N r)\right)^T, \tag{A24}$$

$$\Phi_M = \left(J_0(\lambda_M r) \quad Y_0(\lambda_M r) \quad I_0(\lambda_M r) \quad K_0(\lambda_M r)\right)^T, \tag{A25}$$

where J_i and Y_i are the Bessel functions of the first and second kind of order i, respectively. I_i and K_i are modified Bessel functions of the first and second kind of order i, respectively. The coefficient vectors A_N, A_M are to be determined using the boundary conditions.

Using (A4), (A5), (A6), (A22), and (A23), the boundary forces and moments can be represented in a matrix form that is the function of displacements at the boundary, the magnetic field, and the voltage:

$$F_N = B_N^F A_N + C_N^H H_0 + C_N^V V, \tag{A26}$$

$$F_M = B_M^F A_M + C_M^H H_0 + C_M^V V, \tag{A27}$$

where the force, moment, and displacement vectors at the boundary are defined as

$$F_N = \begin{pmatrix} -r_a N_r(r_a) \\ r_b N_r(r_b) \end{pmatrix}, \quad u_N = \begin{pmatrix} u_R(r_a) \\ u_R(r_b) \end{pmatrix}, \tag{A28}$$

$$F_M = \begin{pmatrix} -r_a M_r(r_a) \\ -r_a R_r(r_a) \\ r_b M_r(r_b) \\ r_b R_r(r_b) \end{pmatrix}, \quad u_M = \begin{pmatrix} \left.\frac{\partial w}{\partial r}\right|_{r=r_a} \\ w(r_a) \\ \left.\frac{\partial w}{\partial r}\right|_{r=r_b} \\ w(r_b) \end{pmatrix}. \tag{A29}$$

The matrices $B_N^F, B_M^F, C_N^H, C_M^H, C_N^V, C_M^V$ are defined in (A30) and (A31), see above, and

$$C_N^H = \gamma_{mN}\begin{pmatrix} -r_a \\ r_b \end{pmatrix}, \tag{A32}$$

$$C_M^H = \gamma_{mM}\begin{pmatrix} -r_a \\ 0 \\ r_b \\ 0 \end{pmatrix}, \tag{A33}$$

$$C_N^V = \gamma_{pN}\begin{pmatrix} -r_a \\ r_b \end{pmatrix}, \tag{A34}$$

$$C_M^V = \gamma_{pM}\begin{pmatrix} -r_a \\ 0 \\ r_b \\ 0 \end{pmatrix}, \tag{A35}$$

Authorized licensed use limited to: Peking University. Downloaded on February 24,2010 at 22:07:09 EST from IEEE Xplore. Restrictions apply.

where J_N^{0a} denotes $J_0(\lambda_N r_a)$, and so on, and α, β are defined as $\alpha = A_{12}/A_{11}$ $\beta = (1 - D_{12}/D_{11})/\lambda_M$.

Similar to the force boundary conditions, the displacement boundary conditions of (A28) and (A29) can be also expressed in a matrix form by using (A22) and (A23)

$$u_N = B_N^u A_N, \tag{A36}$$

$$u_M = B_M^u A_M, \tag{A37}$$

where B_N^u and B_M^u are defined as

$$B_N^u = \begin{bmatrix} J_N^{1a} & Y_N^{1a} \\ J_N^{1b} & Y_N^{1b} \end{bmatrix}, \tag{A38}$$

$$B_M^u = \begin{bmatrix} -\lambda_M J_M^{1a} & -\lambda_M Y_M^{1a} & \lambda_M I_M^{1a} & -\lambda_M K_M^{1a} \\ J_M^{0a} & Y_M^{0a} & I_M^{0a} & K_M^{0a} \\ -\lambda_M J_M^{1b} & -\lambda_M Y_M^{1b} & \lambda_M I_M^{1b} & -\lambda_M K_M^{1b} \\ J_M^{0b} & Y_M^{0b} & I_M^{0b} & K_M^{0b} \end{bmatrix}. \tag{A39}$$

As can be seen in (9), the electric charge of piezoelectric layer has relationship with both the mechanical displacements and the electric voltage. Considering the definitions of C_N^V and C_M^V, the charge can be now expressed as

$$Q = -(C_N^V)^T u_N - (C_M^V)^T u_M + C_0 V. \tag{A40}$$

Appendix B

Circular Bilayer ME Composite

The impedance matrix of a circular bilayer ME composite of the radius r_b can be derived in a similar way. In the case of the circular bilayer ME composite, the general solutions to the equations of motion are expressed in terms of only J_i and I_i because the displacement has a finite value at $r = 0$; the Bessel functions Y_i and K_i go to infinity at $r = 0$:

$$\Phi_N = J_1(\lambda_N r), \tag{B1}$$

$$\Phi_M = \begin{pmatrix} J_0(\lambda_M r) & I_0(\lambda_M r) \end{pmatrix}^T. \tag{B2}$$

The force, moment, and displacement vectors at boundary reduce to:

$$F_N = r_b N_r(r_b), \quad u_N = u_R(r_b), \tag{B3}$$

$$F_M = \begin{pmatrix} r_b M_r(r_b) \\ r_b R_r(r_b) \end{pmatrix}, \quad u_M = \begin{pmatrix} \left.\frac{\partial w}{\partial r}\right|_{r=r_b} \\ w(r_b) \end{pmatrix}. \tag{B4}$$

Following the same procedures as the annular bilayer ME composite, the matrices $B_N^u, B_M^u, B_N^F, B_M^F, C_N^H, C_M^H, C_N^V, C_M^V$ are derived as

$$\begin{aligned} B_N^u &= J_N^{1b}, \quad B_N^F = A_{11}(\lambda_N r_b J_N^{0b} - J_N^{1b} + \alpha J_N^{1b}), \\ C_N^H &= \gamma_{mN} r_b, \quad C_N^V = \gamma_{pN} r_b, \end{aligned} \tag{B5}$$

$$B_M^u = \begin{pmatrix} -\lambda_M J_M^{1b} & \lambda_M I_M^{1b} \\ J_M^{0b} & I_M^{0b} \end{pmatrix}, \tag{B6}$$

$$B_M^F = D_{11}\lambda_M^2 \begin{pmatrix} -r_b J_M^{0b} + \beta J_M^{1b} & r_b I_M^{0b} - \beta I_M^{1b} \\ -\lambda_M r_b J_M^{1b} & -\lambda_M r_b I_M^{1b} \end{pmatrix}, \tag{B7}$$

$$C_M^H = \begin{pmatrix} \gamma_{mM} r_b \\ 0 \end{pmatrix}, \quad C_M^V = \begin{pmatrix} \gamma_{pM} r_b \\ 0 \end{pmatrix}. \tag{B8}$$

References

[1] M. Fiebig, “Revival of the magnetoelectric effect,” *J. Phys. D Appl. Phys.*, vol. 38, pp. R123–R152, Apr. 2005.

[2] R. Ramesh and N. A. Spaldin, “Multiferroics: Progress and prospects in thin films,” *Nat. Mater.*, vol. 6, pp. 21–29, Jan. 2007.

[3] S. W. Cheong and M. Mostovoy, “Multiferroics: A magnetic twist for ferroelectricity,” *Nat. Mater.*, vol. 6, pp. 13–20, Jan. 2007.

[4] C. W. Nan, M. I. Bichurin, S. Dong, and D. Viehland, “Multiferroic magnetoelectric composites: Historical perspective, status, and future directions,” *J. Appl. Phys.*, vol. 103, art. no. 031101, Feb. 2008.

[5] T. Kimura, “Spiral magnets as magnetoelectrics,” *Annu. Rev. Mater. Res.*, vol. 37, pp. 387–413, Aug. 2007.

[6] J. Boomgard, D. R. Terrell, R. A. J. Born, and H. F. J. I. Giller, “An in situ grown eutectic magnetoelectric composite material,” *J. Mater. Sci.*, vol. 9, pp. 1705–1709, Oct. 1974.

[7] M. Avellanedam and G. Harshe, “Magnetoelectric effect in piezoelectric magnetostrictive multilayer (2-2) composites,” *J. Intell. Mater. Syst. Struct.*, vol. 5, pp. 501–513, Jul. 1994.

[8] G. Srinivasan, E. T. Rasmussen, J. Gallegos, R. Srinivasan, Y. I. Bokhan, and V. M. Laletin, “Magnetoelectric bilayer and multilayer structures of magnetostrictive and piezoelectric oxides,” *Phys. Rev. B*, vol. 64, art. no. 214408, Nov. 2001.

[9] J. Ryu, A. Vazquez Carazo, K. Uchino, and H. E. Kim, “Magnetoelectric properties in piezoelectric and magnetostrictive composites,” *Jpn. J. Appl. Phys.*, vol. 40, no. 8, pp. 4948–4951, Aug. 2001.

[10] S. X. Dong, J. F. Li, and D. Viehland, “A longitudinal-longitudinal mode TERFENOL-D/Pb($Mg_{1/3}Nb_{2/3}$)O_3-$PbTiO_3$ laminate composite,” *Appl. Phys. Lett.*, vol. 85, pp. 5305–5306, Nov. 2004.

[11] H. Zheng, J. Wang, S. E. Lofland, Z. Ma, L. Mohaddes-Ardabili, T. Zhao, L. Salamanca-Riba, S. R. Shinde, S. B. Ogale, F. Bai, D. Viehland, Y. Jia, D. G. Schlom, M. Wuttig, A. Roytburd, and R. Ramesh, “Multiferroic $BaTiO_3$-$CoFe_2O_4$ nanostructures,” *Science*, vol. 303, pp. 661–663, Jan. 2004.

[12] W. Eerenstein, M. Wiora, J. L. Prieto, J. F. Scott, and N. D. Mathur, “Giant sharp and persistent converse magnetoelectric effects in multiferroic epitaxial heterostructures,” *Nature Mater.,* vol. 6, pp. 348–351, May 2007.

[13] S. X. Dong, J. Y. Zhai, J. F. Li, and D. Viehland, “Near-ideal magnetoelectricity in high-permeability magnetostrictive/piezofiber laminates with a (2-1) connectivity,” *Appl. Phys. Lett.*, vol. 89, art. no. 252904, Dec. 2006.

[14] S. X. Dong, J. F. Li, and D. Viehland, “Ultrahigh magnetic field sensitivity in laminates of TERFENOL-D and Pb($Mg_{1/3}Nb_{2/3}$))$_3$-$PbTiO_3$ crystals,” *Appl. Phys. Lett.*, vol. 83, pp. 2265–2267, Sep. 2003.

[15] S. X. Dong, J. F. Li, and D. Viehland, “Vortex magnetic field sensor based on ring-type magnetoelectric laminate,” *Appl. Phys. Lett.*, vol. 85, pp. 2307–2309, Sep. 2004.

[16] S. X. Dong, J. Y. Zhai, J. F. Li, D. Viehland, and S. Priya, “Multimodal system for harvesting magnetic and mechanical energy,” *Appl. Phys. Lett.*, vol. 93, art. no. 103511, Sep. 2008.

[17] S. X. Dong, J. F. Li, D. Viehland, J. Cheng, and L. E. Cross, “A strong magnetoelectric voltage gain effect in magnetostrictive-piezoelectric composite,” *Appl. Phys. Lett.*, vol. 85, pp. 3534–3536, Oct. 2004.

[18] S. X. Dong, J. Y. Zhai, J. F. Li, D. Viehland, and M. I. Bichurin, “Magnetoelectric gyration effect in $Tb_{1-x}Dy_xFe_{2-y}$/Pb(Zr,Ti)O_3 laminated composites at electromechanical resonance,” *Appl. Phys. Lett.*, vol. 89, art. no. 243512, Dec. 2006.

[19] A. S. Tatarenko, G. Srinivasan, and M. I. Bichurin, “Magnetoelectric microwave phase shifter,” *Appl. Phys. Lett.*, vol. 88, art. no. 183507, May 2006.

Authorized licensed use limited to: Peking University. Downloaded on February 24,2010 at 22:07:09 EST from IEEE Xplore. Restrictions apply.

[20] Y. K. Fetisov and G. Srinivasan, "Electric field tuning characteristics of a ferrite-piezoelectric microwave resonator," *Appl. Phys. Lett.*, vol. 88, art. no. 143503, Apr. 2006.

[21] S. X. Dong, J. R. Cheng, J. F. Li, and D. Viehland, "Enhanced magnetoelectric effects in laminate composites of Terfenol-D/Pb(Zr,Ti)O_3 under resonant drive," *Appl. Phys. Lett.*, vol. 83, pp. 4812–4814, Dec. 2003.

[22] J. G. Wan, Z. Y. Li, Y. Wang, M. Zeng, G. H. Wang, and J. M. Liu, "Strong flexural resonant magnetoelectric effect in Terfenol-D/epoxy-Pb(Zr,Ti)O_3 bilayer," *Appl. Phys. Lett.*, vol. 86, art. no. 202504, May 2005.

[23] Z. P. Xing, S. X. Dong, J. Y. Zhai, L. Yan, J. F. Li, and D. Viehland, "Resonant bending mode of Terfenol-D/steel/Pb(Zr,Ti)O_3 magnetoelectric laminate composites," *Appl. Phys. Lett.*, vol. 89, art. no. 112911, Sep. 2006.

[24] J. Y. Zhai, S. X. Dong, Z. P. Xing, J. F. Li, and D. Viehland, "Giant magnetoelectric effect in Metglas/polyvinylidene-fluoride laminates," *Appl. Phys. Lett.*, vol. 89, art. no. 083507, Aug. 2006.

[25] L. Li and X. M. Chen, "Magnetoelectric characteristics of a dual-mode magnetostrictive/piezoelectric bilayered composite," *Appl. Phys. Lett.*, vol. 92, art. no. 072903, Feb. 2008.

[26] V. M. Petrov, G. Srinivasan, M. I. Bichurin, and T. A. Galkina, "Theory of magnetoelectric effect for bending modes in magnetostrictive-piezoelectric bilayers," *J. Appl. Phys.*, vol. 105, art. no. 063911, Mar. 2009.

[27] M. S. Guo and S. X. Dong, "A resonance-bending mode magnetoelectric-coupling equivalent circuit," *IEEE Trans. Ultrason. Ferroelectr. Freq. Control*, vol. 56, pp. 2578–2586, Nov. 2009.

[28] S. X. Dong, J. F. Li, and D. Viehland, "Circumferentially magnetized and circumferentially polarized magnetostrictive/piezoelectric laminated rings," *J. Appl. Phys.*, vol. 96, pp. 3382–3387, Sep. 2004.

[29] S. K. Ha and Y. H. Kim, "Impedance and admittance matrices of symmetric piezoelectric annular bimorphs and their applications," *J. Acoust. Soc. Am.*, vol. 108, pp. 2125–2133, Nov. 2000.

[30] S. K. Ha and Y. H. Kim, "Analysis of an asymmetrical piezoelectric annular bimorph using impedance and admittance matrices," *J. Acoust. Soc. Am.*, vol. 110, pp. 208–215, Jul. 2001.

[31] J. Yang, Comment on "Admittance matrix of asymmetric piezoelectric bimorph with two separate electric ports under general distributed load," *IEEE Trans. Ultrason. Ferroelectr. Freq. Control*, vol. 54, pp. 1087–1089, Jun. 2007.

[32] Z. Fang, S. G. Lu, F. Li, S. Datta, Q. M. Zhang, and M. El Tahchi, "Enhancing the magnetoelectric response of Metglas/polyvinylidene fluoride laminates by exploiting the flux concentration effect," *Appl. Phys. Lett.*, vol. 95, art. no. 112903, Sep. 2009.

[33] Ferroperm materials data. [Online]. Available: http://www.ferroperm-piezo.com.

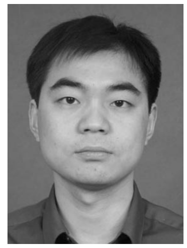

Mingsen Guo was born in 1980 at Hubei, China. He received the B.Sc. degree in physics, M.Sc. degree in physics of condensed matter, and Ph.D. degree in physics and chemistry of materials from Wuhan University, Wuhan, China, in 2002, 2005, and 2008, respectively. He is currently a postdoctoral fellow at Peking University, Beijing, China. From December 2005 to October 2007, he was a research assistant at Hong Kong Polytechnic University, HK SAR, China. His main research interests include piezoelectric materials, sensors, and actuators.

Shuxiang Dong (M'03) is a professor of advanced materials and nanotechnology at the College of Engineering at Peking University, Beijing, China. He received his B.S. degree in semiconductor physics from Wuhan University, Wuhan, China, in 1982 and his M.S. degree in acoustics physics and Ph.D. degree in electronic materials and devices from Tsinghua University, Beijing, China, in 1989 and 1993, respectively. Dr. Dong was a recipient of a first place award at the 2000 Advances in Materials Poster at Materials Research Laboratory, Pennsylvania State University, State College, PA. He has authored more than 80 peer-reviewed papers and holds 13 patents. His research interests include transducers and sensors, piezoelectric actuators and ultrasonic motors, and other functional devices.

Authorized licensed use limited to: Peking University. Downloaded on February 24,2010 at 22:07:09 EST from IEEE Xplore. Restrictions apply.